Radiometric calibration of the vacuum-ultraviolet spectrograph SUMER on the SOHO spacecraft with the B detector

Udo Schühle, Werner Curdt, Jörg Hollandt, Uri Feldman, Philippe Lemaire, and Klaus Wilhelm

The Solar Ultraviolet Measurement of Emitted Radiation (SUMER) vacuum-ultraviolet spectrograph was calibrated in the laboratory before the integration of the instrument on the Solar and Heliospheric Observatory (SOHO) spacecraft in 1995. During the scientific operation of the SOHO it has been possible to track the radiometric calibration of the SUMER spectrograph since March 1996 by a strategy that employs various methods to update the calibration status and improve the coverage of the spectral calibration curve. The results for the A Detector were published previously [Appl. Opt. **36,** 6416 (1997)]. During three years of operation in space, the B detector was used for two and one-half years. We describe the characteristics of the B detector and present results of the tracking and refinement of the spectral calibration curves with it. Observations of the spectra of the stars α and ρ Leonis permit an extrapolation of the calibration curves in the range from 125 to 149.0 nm. Using a solar coronal spectrum observed above the solar disk, we can extrapolate the calibration curves by measuring emission line pairs with well-known intensity ratios. The sensitivity ratio of the two photocathode areas can be obtained by registration of many emission lines in the entire spectral range on both KBr-coated and bare parts of the detector's active surface. The results are found to be consistent with the published calibration performed in the laboratory in the wavelength range from 53 to 124 nm. We can extrapolate the calibration outside this range to 147 nm with a relative uncertainty of ±30% (1σ) for wavelengths longer than 125 nm and to 46.5 nm with 50% uncertainty for the short-wavelength range below 53 nm.

OCIS codes: 120.5630, 120.6200, 300.6190, 300.6540.

1. Introduction

The vacuum-ultraviolet spectrograph Solar Ultraviolet Measurement of Emitted Radiation[1] (SUMER) on the Solar and Heliospheric Observatory (SOHO) measures the emission from the solar atmosphere in the wavelength range from 46.5 to 161.0 nm with high spatial and spectral resolution. With careful radiometric calibration performed in the laboratory[2] before delivery of the instrument to the SOHO payload, and by tracking of the calibration during the flight,[3] the instrument was used to measure absolute radiance of the Sun in the entire spectral range and even of full-Sun irradiances in many spectral lines.[4] After observation of the first light on 24 January 1996 the instrument was operated continuously with the prime detector (A detector), and the radiometric calibration was traced from laboratory calibration to in-flight conditions by methods described in previous publications.[5,6] After 24 September 1996 it was decided to switch the instrument configuration to operate the B detector, while the A detector was put into a resting state. Since then the B detector has been operative for most of the time. We show here how the radiometric calibration of the SUMER instrument with the B detector was maintained during flight and give detailed descriptions of the methods employed to refine the spectral calibration curves. First we give some instrumental details that are pertinent to the calibration of SUMER data obtained with the B detector. Then the different measure-

U. Schühle (schuehle@linmpi.mpg.de), W. Curdt, and K. Wilhelm are with the Max-Planck-Institut für Aeronomie, D-37191 Katlenburg-Lindau, Germany. J. Hollandt is with the Physikalisch-Technische Bundesanstalt, D-10587 Berlin, Germany. U. Feldman is with the Naval Research Laboratory, Washington, D.C. 20375. P. Lemaire is with the Institut d'Astrophysique Spatiale, Unité Mixte Centre National de la Recherche Scientifique, Université Paris XI, Batiment 121, F-91405 Orsay, France.

Received 24 May 1999; revised manuscript received 20 September 1999.

0003-6935/00/030418-08$15.00/0

ments performed to refine the calibration curves are described and analyzed. Finally we present the instrument sensitivity curves obtained and discuss their accuracy.

2. SUMER Instrument with the B Detector

The optical elements of the telescope and spectrograph are made from silicon carbide (SiC) with a chemical-vapor-deposited SiC coating. Even with this surface the short-wavelength useful efficiency of the instrument is restricted to wavelengths greater than approximately 46.5 nm. As a result, practically only first- and second-order spectra are observed because of the low efficiency of the mirrors at short wavelengths (few third-order lines have been identified). The spectrum produced by the concave grating is registered by two imaging detectors: the A detector is mounted in a strict Wadsworth configuration, whereas the B detector is offset from the grating normal by 2.4°. Thus the total wavelength ranges of the two detectors are slightly different: The A detector covers 78.0–161.0 nm in first order (39.0–85.0 nm in second order) and the B detector first-order range extends from 66.0 to 150.0 nm (33.0–75.0 nm in second order). For the B detector there is a larger overlapping wavelength range of first- and second-order spectra than for the A detector. The detector format consists of 360 spatial and 1024 spectral pixels. The photocathode of the B detector is coated with potassium bromide (KBr) for spectral pixels 270 to 758. The remainder of the array exposes the bare microchannel plate. In addition, there is an attenuating mask (1:10) in front of spectral pixels 23–53 and 970–1005. [The pixel numbers given above are those of instrument pixels; SUMER data are normally converted to copixels = 1023 minus the pixel number.] The small offset angle of the B detector position leads to small differences in the spectral dispersion value and the spatial magnification of the spectrometer, which have to be considered when instrument count rates are transformed into physical units. A radiometric calibration routine supplied for SUMER data takes these factors into account.

3. Laboratory Calibration and Application with SOHO

The radiometric calibration performed before the flight of the SOHO has been described in detail.[2] In brief, the radiometric sensitivity of the SUMER instrument was calibrated with a hollow-cathode discharge source as a transfer standard that was calibrated against the Berlin electron-storage ring for synchrotron radiation (BESSY I), a primary radiometric source standard. By use of the bright emission lines of inert gases of the hollow-cathode source, the sensitivity of the instrument was measured at various wavelengths in the spectral range from 53.7 to 147.0 nm. Both detectors had to be calibrated independently. For each emission line of the source the calibration was performed at three positions on the photocathode of each detector. An average was taken over a large part of the detector's active surface

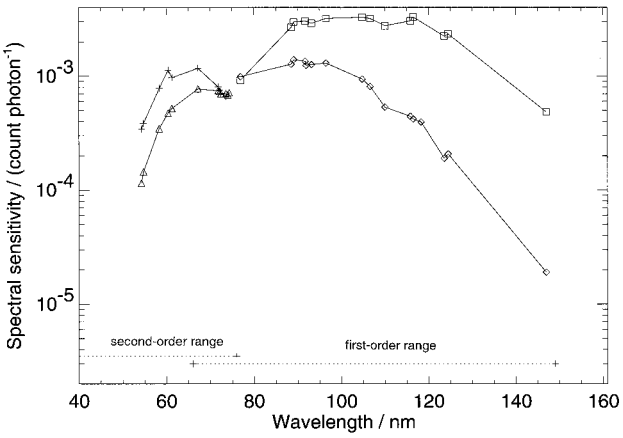

Fig. 1. Results of the laboratory calibration of the SUMER spectrograph with the B detector obtained with the lines of inert gases of the hollow-cathode source. The data points for KBr and for the bare photocathodes are connected by solid curves when they are observed in the first or the second order separately. The aperture area of the SUMER instrument is 117 cm^2.

to neutralize the well-known effects of small-scale nonuniformities of microchannel plate detectors. The relative uncertainty of the radiometric calibration on ground is 12% (1σ) in the wavelength range covered.[2] Figure 1 shows the results of the laboratory calibration of SUMER with the B detector.

The fixed pattern of efficiency differences given by the small-scale nonuniformities of the channel plate gain can be removed to a large extent by flat-field correction. Quasi-flat-field images have been produced regularly (approximately every two months) during the operational phase with the Lyman continuum of the Sun as the source and the spectrometer in an unfocused position. An onboard routine produces the flat-field correction matrix from these data by extracting the features smaller than 16 $\times$ 16 pixels with a median filter, resulting in a relative sensitivity matrix scaled from 0.5 to 1.5. In Fig. 2 we show the correction matrix derived from this quasi-flat illumination. Both images are telemetered to the ground station for flat-field treatment of data on the ground (or even to undo the flat-field correction if it had been made onboard).

Under normal operating conditions on the SOHO, with observations on the solar disk, the detector is used permanently at a high count rate close to saturation of the channel plates and the image-processing electronics. When bright solar lines are being observed, the local gain of the channel plates saturates, depending on the local count rate. If the global count rate of the detector exceeds 10^4 counts/s, the dead-time effects of the position-encoding electronics must be considered. Both effects, the local gain depression and the electronic dead-time effects, were studied during the laboratory calibration[1] and by measurements in flight,[5] and by use of these results, they can be corrected accordingly.

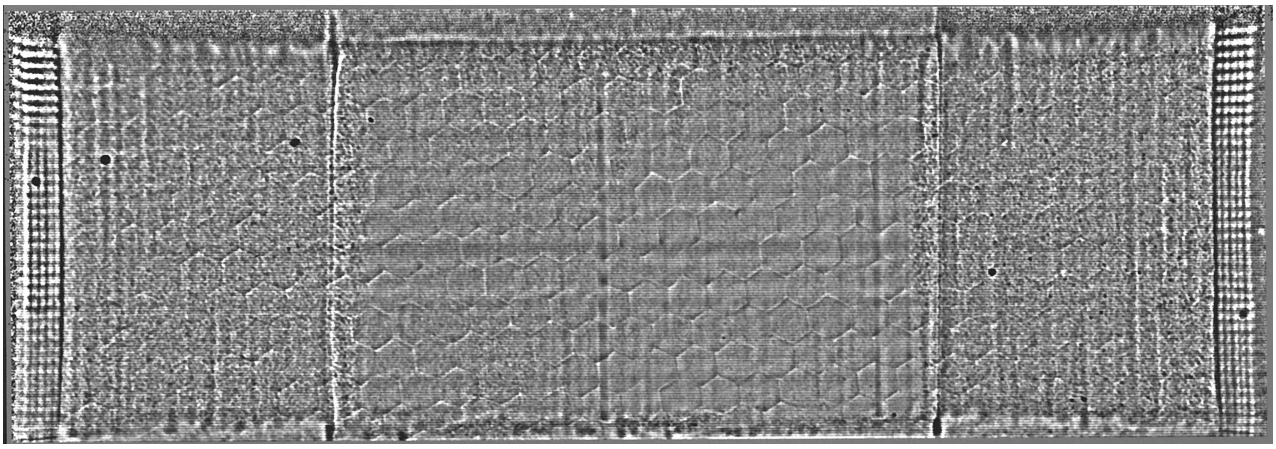

Fig. 2. Flat-field correction matrix used to correct small-scale fixed pattern features of the microchannel plate detector. The matrix contains the relative pixel sensitivity values from 0.5 to 1.5. The data array was extracted with a median filter of 16 × 16 pixels from quasi-flat illumination of the detector's field of view.

4. Stability of the Calibration of the B Detector

When the observational configuration of the SUMER instrument was switched from the A detector to the B detector, a comparison of the sensitivity was made with both detectors. Because the A detector had been stable during the time of its use (see Ref. 3), the calibration could be transferred, and the initial calibration of the B detector was confirmed. To track the stability of the spectral sensitivity of the SUMER instrument during the operational phase, regular observations were made of selected emission lines in quiet-Sun regions (neither active regions nor coronal holes) near the center of the solar disk. These observations are part of the intercalibration programs aimed at cross calibrations between the ultraviolet instruments on the SOHO. These measurements were made with the emission lines of He I at 58.4 nm, Mg X at 60.9 and 62.4 nm, Ne VIII at 77.0 nm, and N V at 123.8 nm. In addition, regular measurements of the intensity of the Lyman continuum at 88.0 nm were made. The cross calibration with the other ultraviolet instruments of the SOHO will be the subject of a separate publication[7]; here we use the data obtained to monitor the stability of the SUMER calibration. A detailed description of the measurement procedure can be found in Ref. 3. From these measurements we deduce the mean solar radiance of the emission lines in the observed area by integrating the line profiles and separating them from background and continuum emission. In Figure 3 we summarize the results of the radiance measurements performed with the B detector since 28 August 1996. The actual dates of measurements are indicated. Variations of the radiances of as much as 30% in the observed quiet-Sun emission lines are larger than statistical uncertainties and are accounted for by local changes in the solar emission. A linear fit to the data set of each line shows that no loss in the sensitivity of the instrument has occurred at these wavelengths. Rather, a general increase of intensity can be observed in all lines. This increase is coincident with the solar activity cycle and is less pronounced in the optically thick He I line. Thus we conclude that these variations are not an instrumental effect.

During the long period of operation, the detector microchannel plates suffer from aging. Because of the large amount of charge extracted from the channel plates, the gain is being reduced, and an increase in operating voltage is needed to keep the gain at the required level. For this reason, the pulse height distribution (PHD) of the detector output pulses was monitored during data acquisition times; whenever the PHD decreased to a level such that 10% of the counts fell below the discriminator threshold, the channel plate's high voltage was raised to compensate for the gain loss. The PHD measurement was always performed at the wavelength of the Lyman continuum at 88.0 nm, which produces a nearly uniform count rate over the whole detector area; thus the PHD can be sampled uniformly.

Local gain depletion could not be avoided in this way, but the distribution of the aging was determined largely by the way in which the instrument was operated: The instrument software allows us to place the selected spectral range at any pixel location, so we could prevent detection of intense lines at the same pixel location for long time periods. A cumulative history of representatively sampled counts in certain pixel areas that is held in the data memory and sent to ground on demand is used to verify this. In Fig. 4 we show such an image of the history memory, which represents a map of all detected counts on the detector from the beginning of its operation during laboratory calibration until June 1998. The top panels show the average counts per column (left) and row (right) of the memory history shown in the lower panel. From the distribution of counts we see that no local area on the detector has been used extensively or was starved of counts and that the detector was used more-or-less evenly. Clearly, the central columns correspond to the KBr photocathode with its higher efficiency and the central rows correspond to

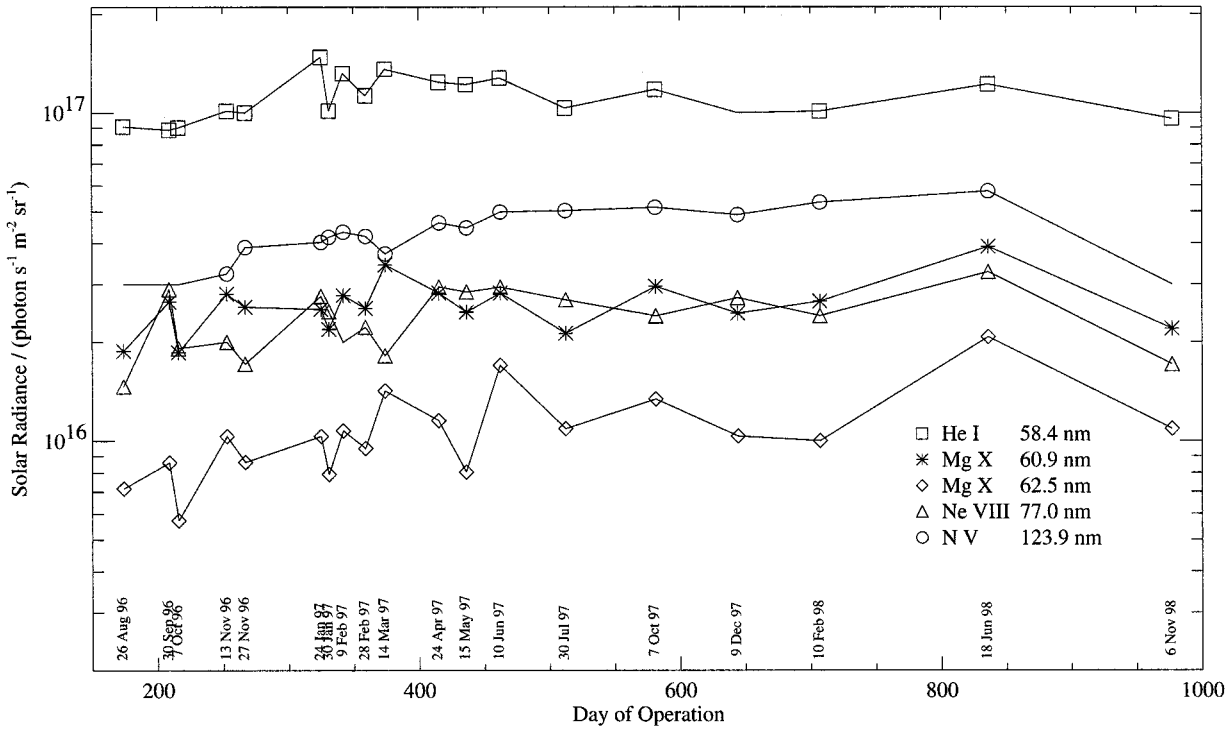

Fig. 3. Radiances of the emission lines of He I (58.4 nm), Mg X (60.9 and 62.5 nm), Ne VIII (77.0 nm), and N V (123.9 nm) measured during several calibration runs between 28 August 1996 and 6 November 1998. The actual dates of the measurements are given at the bottom.

the short spectrometer slit of 120 arcsec in the centered position (the off-center positions of the slit have not been used so much). The upper and lower edges are not sharp because the residual inclination of the grating and scan mechanism results in a vertical movement of the spectrum that depends on the wavelength selected. Thus, only the areas under the attenuators and the extreme upper and lower edges of the active photocathode surface stay less used, and we can expect high gain at these locations.

To minimize the aging of the detector, we decided to lower the high voltage to a parking level of −3000 V whenever no data were acquired. When the B detector was activated on 24 September 1996, we decided to reduce the aging further by operating the detector at the lowest gain possible without losing counts in the discriminator stage. This had the effect that the PHD was always close to the discriminator threshold, and any loss of gain would result in a loss of counts. Thus a variation of ±7% of detector efficiency between adjustments of the high voltage could not be prevented and must enter the uncertainty budget whenever data are calibrated.

During the course of operations, the high voltage of the detector was raised from initially 4700 V to the current 5560 V, and a total number of 3×10^{11} counts was collected. In Figure 5 the history of the B detector is summarized, showing the total accumulated counts versus time and the high voltage increase with the number of accumulated counts. It seems that, finally, the aging of the channel plates is reaching a level at which fewer high-voltage increments are needed. It must be noted here that only the possibility to distribute the total counts evenly on the detector active surface allowed us to increase the high voltage sequentially for compensation of the gain loss over such a large range and, thus, to keep the SUMER instrument in a calibrated mode.

The aging also has a small effect on the fixed pattern of the flat-field image: The change in channel plate gain produces a small shift of position of the fixed pattern. This shift is generally less than half a pixel in two months, depending on the average total counts during the time period. Therefore, approximately every two months, whenever a gain adjustment was necessary, the flat-field image was replaced. However, the usage of the detector active surface during such a time is not uniform, and thus a differential shift can remain uncorrected, which limits the performance of this flat-field routine.

5. Refinement of the Calibration during the SOHO Mission

Despite the successful initial calibration and the overall stability during flight, the spectral calibration curve was based on a set of bright emission lines of the inert gases (53.7–146.9 nm) provided by the calibration source used during the laboratory calibration. This approach left significant gaps between those lines, particularly from 54.8 to 71.8 nm and from 123.5 and 146.9 nm. To verify and complement the laboratory calibration and fill the gaps in the calibration curves, we used different methods to arrive at the data with the Sun and bright UV stars as

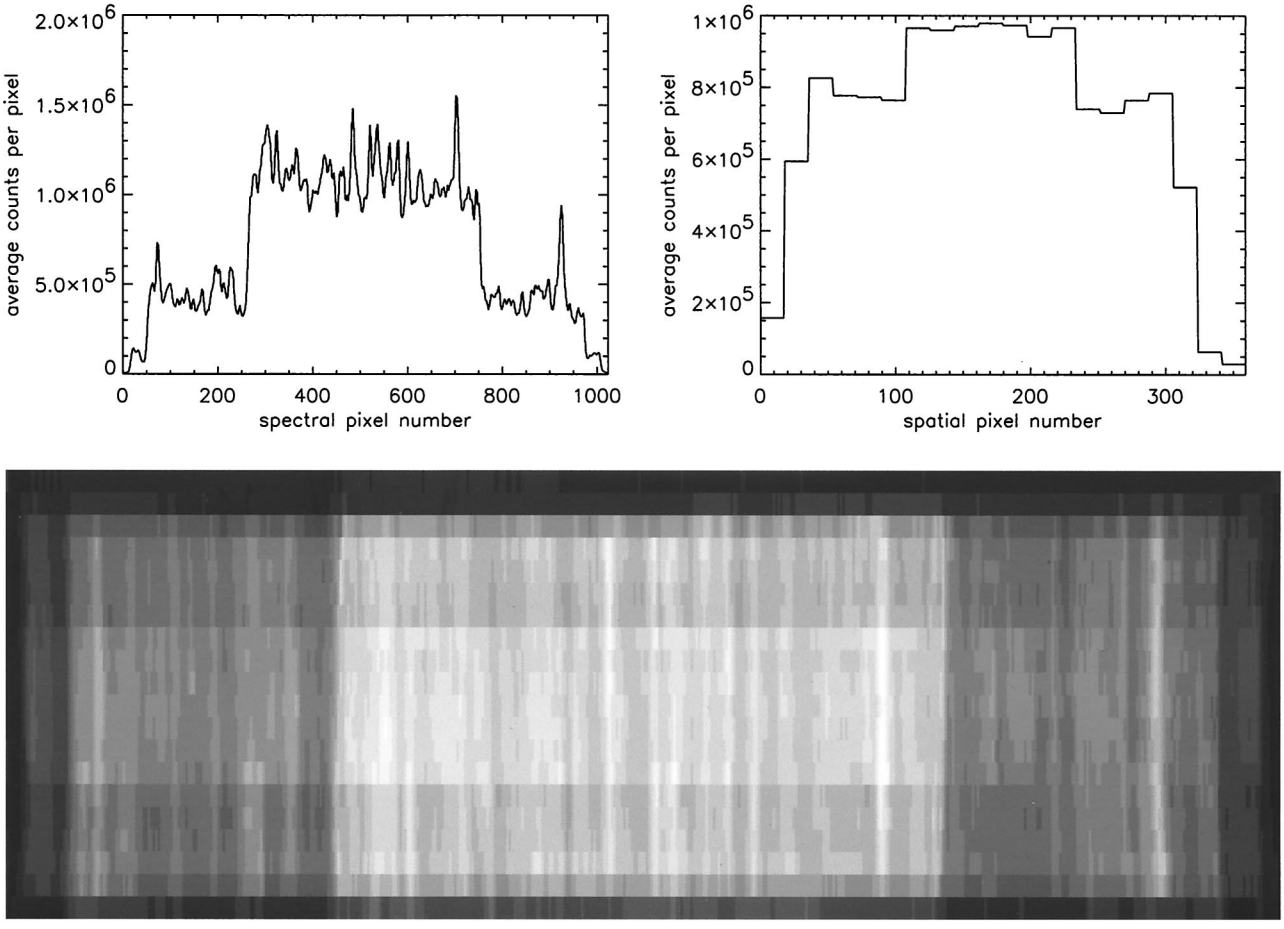

Fig. 4. History memory data of the B detector as of June 1998: column (top left) and row (top right) averages and map of the total accumulated counts per pixel on the detector active area (lower panel).

the sources. Most of the data were acquired by a reference spectrum, an observing sequence that provides a full spectral scan of the spectrometer. Such a spectrum consists of 62 images displaced by a spectral increment of 1.27 nm from one to the next. In such a way it is possible to record each part of the spectrum once on the bare and once on the KBr sections of the photocathode. For this purpose a spectrum was chosen in which the slit position was pointed above the solar limb above an active region, which provided intense hot streamer plasma with many spectral lines of high-temperature species and less continuum emission. This procedure guaranteed that the observed lines did not vary much during the time of the measurement, and continuum contributions to line intensities were negligible. The spectral lines were identified from the spectral atlases of Curdt *et al.*[8] and Feldman *et al.*[9]

A. Spectrometer Efficiency Ratios in First and Second Orders

With the B detector the range of overlapping orders is larger than for the A detector, thus allowing us to determine the grating efficiency ratio by observing the same lines in both the first and the second orders of the spectrometer. In the range from 67.6 to 72.1 nm we identified 12 lines that we could observe in both orders. The intensities of lines were determined by integration of the intensity along the slit length and by fitting of a Gaussian to the line profile with continuum subtraction. Where it was necessary, a multi-Gauss fit was used to separate the lines from blends. In Table 1 we have compiled the results of the measured sensitivity ratios. The variation of the results is as large as 20% and is caused by the variation of the emission of the observed target. But, as we can assume that the grating efficiency in this wavelength range is not a steep function, we can fit a linear function to the data. We find that the grating efficiency ratio varies from 0.9 at 67 nm to 1.3 at 72 nm. Starting from the laboratory calibration points for the bare photocathode in second order, where we have good coverage of data points (see Fig. 1), we can transfer these data to the first-order curve to extrapolate the bare photocathode calibration in first order to shorter wavelengths from 88.9 to 67 nm with a gap from 88.9 to 76.9 nm. Within this gap the efficiency of the bare part is not a steep function and varies from 9.9×10^{-4} to 12.7×10^{-4}; thus a linear interpolation in this range will be a good approximation. The efficiency of the KBr is a steep function in this same range, and therefore we use the KBr-to-

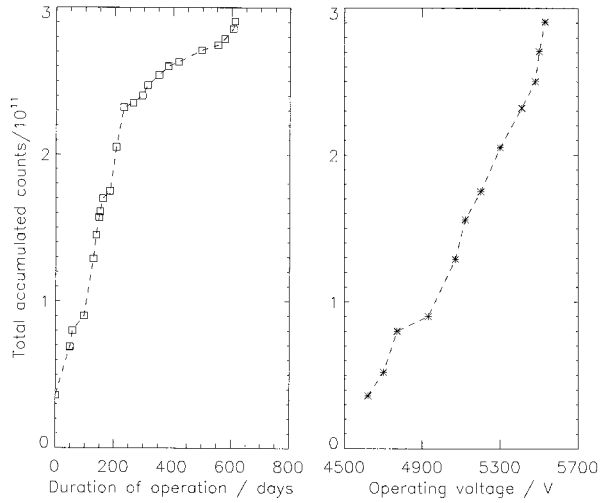

Fig. 5. History of the B detector total accumulated counts versus time of operation and the evolution of the high-voltage increments versus accumulated counts.

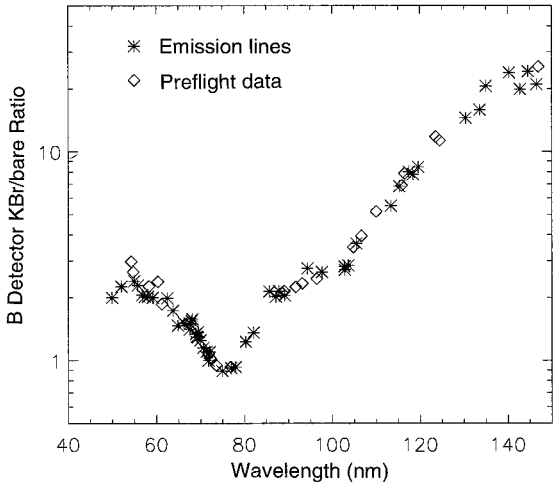

Fig. 6. Ratio of the two photocathode efficiencies KBr/bare. The laboratory calibration data are included for comparison with the flight data.

bare ratio, which we can measure with better accuracy, to transfer the calibration in the range so far covered from the bare to the KBr-coated parts.

B. Photocathode Sensitivity Ratios

It is crucial for good accuracy in the line intensity measurements that the solar radiation observed not vary much in space and time. This requirement limits the accuracy of the first- to the second-order efficiency ratio presented above because the lines observed in both orders lie at the opposite extremes of the SUMER spectrum, which separates their time of observation as much as 5 h, given the observing sequence used to acquire this spectrum. All lines, however, are observed on the KBr and bare parts in sequence with a separation of only 5 min. As a result, many more lines can be used for determination of this ratio, and the accuracy of their measurement is better. For this measurement, lines were chosen that gave a good fit to a single Gaussian function to eliminate any blends or continuum contributions from other orders. The results are plotted in Fig. 6, together with the ratios obtained from the preflight calibration points. We see that the preflight ratios fit these flight data very well. By fitting a smooth curve to these data we obtain an accurate curve for the KBr-to-bare ratio, which we can use to transfer the calibration from the bare to the KBr photocathode. In particular, the fit will extend the first-order–KBr curve down to 67 nm and fill the gaps in this curve that lie from 88.9 to 76.9 nm and the gaps in the second-order–KBr curve that lie from 67.2 to 71.8 nm.

Table 1. Line Ratios Measured in First and Second Orders

Line	Wavelength (nm)	Ratio, First to Second Orders
Si IX	67.65	1.11
Al IX	68.04	0.88
Na IX	68.17	0.88
Mg VII	68.96	0.90
Ca IX	69.14	1.27
Na IX	69.42	1.13
Si IX	69.47	1.00
Ar VIII	70.02	1.06
Mg IX	70.61	1.10
Ar VIII	71.38	1.10
O II	71.85	1.40
[a]	72.13	1.30

[a]Unidentified line

C. Line-Pair Intensity Ratios

The spectrum analyzed above also contains spectral lines whose theoretical intensity ratios are well known and do not depend significantly on the electron temperature or the electron density. As we have done for the A detector,[6] we can use these line ratios to extrapolate the calibration curves to shorter wavelengths beyond the range of the laboratory calibration. We use the line ratios of Ca X, 57.40/55.77 nm; Al XI, 56.82/55.00 nm; Si XII, 52.07/49.94 nm; and Ne VII, 89.52/46.52 nm with their theoretical intensity ratios listed in Table 2 of Wilhelm *et al.*[6] Except for the Si XII line pair, all pairs have the longer-wavelength emission line inside the range of the laboratory calibration. So we normalize the intensity of these lines to the corresponding sensitivity of the laboratory calibration. We use a linear interpolation between the laboratory calibration points for this procedure and in this way determine the sensitivity at the corresponding shorter wavelength. The results are shown in Fig. 7, with the line designations labeled accordingly. For the Si XII line pair we can use the ratio of the line pairs to determine only the slopes of the curves near 50 nm. The shortest wavelength observed is the Ne VII 46.52-nm line. Its intensities on the bare and KBr photocathodes can be determined only with a low degree of accuracy be-

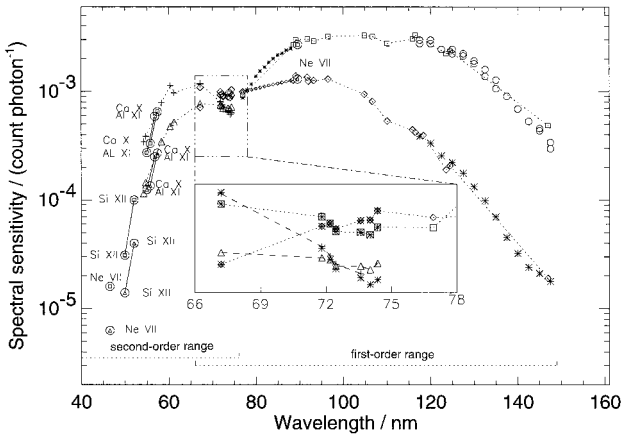

Fig. 7. Radiometric sensitivity data of the SUMER instrument with the B detector from laboratory and flight calibrations. Data symbols for the laboratory points are as in Fig. 1. The region of overlap of first and second orders is magnified in the inset (with the sensitivity scale increased by a factor of 3). Open circles, star observation data. Asterisks, transfer of data by use of KBr/bare or first/second-order ratios. Line ratio data are marked by labels and symbols with open circles.

cause of blends in first order from hydrogen and helium lines. Thus the accuracy of this extrapolation is fairly poor, and for the wavelengths below 50 nm we can only estimate the uncertainty to be 50% (see Fig. 8).

D. Star Observations

To refine the calibration curves at wavelengths above 123.6 nm we used the ability of SUMER to observe stars passing through the field of view within two solar radii. The bright UV stars α Leonis and ρ Leonis, which are used as standard stars for the Hubble Space Telescope,[10] were observed with the B detector on 22 and 28 August 1997, respectively. Their spectral radiances taken from the International Ultraviolet Explorer data are given with uncertainties of 10–15% (1σ). We compared the data with our measurements in first order of the KBr part of the photocathode at wavelengths from 120.0 to 147.5 nm and found good agreement with our calibration at 123.6 nm. Hence these data were used as the baseline for the calibration of the KBr part of the SUMER above 123.6 nm. We used the ratio of the KBr photocathode to the bare microchannel plate to determine the spectral sensitivity of the bare part in the same wavelength range. The resulting data points are included in Fig. 7 as circles in the KBr curve and stars in the bare curve above 120 nm.

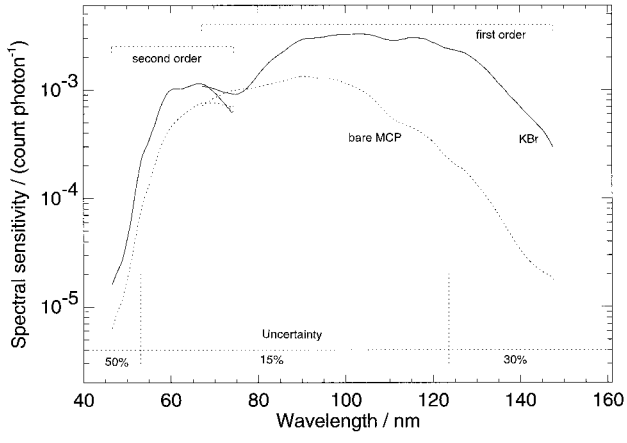

Fig. 8. Refined spectral sensitivity for the SUMER instrument with the B detector. The curves were derived by interpolation between data points and smoothing. The relative uncertainties are valid for the KBr and bare curves and include contributions from optical stops and diffraction losses. MCP, microchannel plate.

6. Summary and Discussion

Using various observational methods, we improved the spectral calibration curves of the SUMER with the B detector. The calibrated range could be extended to wavelengths as short as 46.52 nm by the line ratio method and as long as 147.5 nm by observations of reference stars. By observation of a coronal emission spectrum it was possible to derive accurate ratios of the two photocathode areas and the first- to the second-order efficiency of the spectrometer in the overlapping wavelength range. This allowed us to relate the four calibration curves to one another and to interpolate inside the gaps left by the laboratory calibration. The combination of all data displayed graphically in Fig. 7 shows the consistency of the various measurements and excellent agreement between the flight calibration and the laboratory results obtained two and a half years earlier.

One discrepancy between the laboratory and the star calibrations, however, is evident at 147 nm: The laboratory value of the KBr curve is higher by ~60%. The fact that the laboratory value for the bare curve fits well with the flight values obtained from star observations and KBr-to-bare ratio measurements can indicate that the efficiency of the KBr coating might have decreased at the longest wavelengths. However, from these measurements we cannot conclusively determine whether the one data point of the laboratory measurement was faulty or whether a change in sensitivity has occurred. For determination of the final in-flight calibration curves we shall disregard this one data point for the KBr.

As a summary—and as a database for actual calibration of the SUMER data—we produce from all laboratory and flight calibration results a set of spectral sensitivity curves that provide calibration values throughout the useful spectral range of the SUMER instrument. The curves shown in Fig. 8 were produced by interpolation among all data points and smoothing. They can be used as a basis to convert SUMER data into radiometric units. A conversion program that includes the influence of the apertures is available on the Internet: http://sohowww.nascom.nasa.gov/descriptions/experiments/sumer/radcal.html.

The good agreement between laboratory and flight data gives us confidence that the uncertainty of 12%

in the laboratory calibration is still valid within the range of 53.0–123.6 nm. However, the operation of the B detector close to the discriminator threshold and the nonuniform aging across the active detector area introduce additional variation and uncertainty in the detector efficiency. The corresponding changes in the pulse height distribution and the fact that high-voltage adjustments could be done only stepwise lead to an additional uncertainty, which we estimate to be ±7%. The uncertainty in the main spectral range can thus be safely set to 20% (1σ). In the extrapolated range the uncertainty levels are higher: Above 123.6 nm we rely on the calibration of standard stars, and we estimate the uncertainty of our measurements to be 30%, whereas in the short-wavelength range below 53.0 nm we have only the Ne VII 46.5 nm line, which we could measure with only 50% confidence. More dedicated measurements at these extreme wavelengths and repeated observations of the stars are necessary to improve these results.

SOHO is a project of international cooperation between the European Space Agency (ESA) and the National Aeronautics and Space Administration (NASA). The SUMER project is financially supported by the Deutsches Zentrum für Luft- und Raumfahrt (DLR), the Centre National d'Etudes Spatiales (CNES), NASA, and the ESA PRODEX program (Swiss contribution).

References

1. K. Wilhelm, W. Curdt, E. Marsch, U. Schühle, P. Lemaire, A. Gabriel, J.-C. Vial, M. Grewing, M. C. E. Huber, S. D. Jordan, A. I. Poland, R. J. Thomas, M. Kühne, J. G. Timothy, D. M. Hassler, and O. H. W. Siegmund, "SUMER—solar ultraviolet measurements of emitted radiation," Sol. Phys. **162,** 189–231 (1995).
2. J. Hollandt, U. Schühle, W. Paustian, W. Curdt, M. Kühne, B. Wende, and K. Wilhelm, "Radiometric calibration of the telescope and ultraviolet spectrometer SUMER on SOHO," Appl. Opt. **35,** 5125–5133 (1996).
3. U. Schühle, P. Brekke, W. Curdt, J. Hollandt, P. Lemaire, and K. Wilhelm, "Radiometric calibration tracking of the vacuum-ultraviolet spectrometer SUMER during the first year of the SOHO mission," Appl. Opt. **37,** 2646–2652 (1998).
4. K. Wilhelm, P. Lemaire, I. E. Dammasch, J. Hollandt, U. Schühle, W. Curdt, T. Kucera, D. M. Hassler, and M. C. E. Huber, "Solar irradiances and radiances of UV and EUV lines during the minimum of the sunspot activity in 1996," Astron. Astrophys. **334,** 685–702 (1998).
5. K. Wilhelm, P. Lemaire, W. Curdt, U. Schühle, E. Marsch, A. I. Poland, S. D. Jordan, R. J. Thomas, D. M. Hassler, M. C. E. Huber, J.-C. Vial, M. Kühne, O. H. W. Siegmund, A. Gabriel, J. G. Timothy, M. Grewing, U. Feldman, J. Hollandt, and P. Brekke, "First results of the SUMER telescope and spectrometer on SOHO. I. Spectra and spectroradiometry," Sol. Phys. **170,** 75–104 (1997).
6. K. Wilhelm, P. Lemaire, U. Feldman, J. Hollandt, U. Schühle, and W. Curdt, "Radiometric calibration of SUMER: refinement of the laboratory results under operational conditions on SOHO," Appl. Opt. **36,** 6416–6422 (1997).
7. A. Pauluhn, I. Rüedi, S. K. Solanki, J. Lang, C. D. Pike, U. Schühle, W. T. Thompson, and M. C. E. Huber, "Intercalibration of SUMER and CDS on SOHO. I. SUMER detector A and CDS NIS," Appl. Opt. **38,** 7035–7046 (1999).
8. W. Curdt, U. Feldman, J. M. Laming, K. Wilhelm, U. Schühle, and P. Lemaire, "The solar disk spectrum between 660 and 1175 (first order) obtained by SUMER on SOHO," Astron. Astrophys. Suppl. Ser. **126,** 281–296 (1997).
9. U. Feldman, W. E. Behring, W. Curdt, U. Schühle, K. Wilhelm, P. Lemaire, and T. M. Moran, "A coronal spectrum in the 500–1600 Å wavelength range recorded at a height of 21,000 kilometers above the west solar limb by the SUMER instrument on Solar and Heliospheric Observatory," Astrophys. J. Suppl. Ser. **113,** 195–219 (1997).
10. R. C. Bohlin, A. W. Harris, A. V. Holm, and C. Gry, "The ultraviolet calibration of the Hubble Space Telescope. IV. Absolute IUE fluxes of Hubble Space Telescope standard stars," Astrophys. J. Suppl. Ser. **73,** 413–439 (1990).